

Functional Crosstalk between Bmi1 and MLL/Hoxa9 Axis in Establishment of Normal Hematopoietic and Leukemic Stem Cells

Lan-Lan Smith,¹ Jenny Yeung,^{1,6} Bernd B. Zeisig,^{1,6} Nikolay Popov,^{2,6} Ivo Huijbers,^{3,6} Josephine Barnes,¹ Amanda J. Wilson,¹ Erdogan Taskesen,⁴ Ruud Delwel,⁴ Jesús Gil,² Maarten Van Lohuizen,³ and Chi Wai Eric So^{1,5,*}

¹Leukaemia and Stem Cell Biology Lab, Department of Haematological Medicine, King's College London, London SE5 9NU, UK

²Cell Proliferation Group, MRC Clinical Sciences Centre, Imperial College Faculty of Medicine, Hammersmith Hospital Campus, Du Cane Road, London W12 0NN, UK

³Division of Molecular Genetics and The Centre for Biomedical Genetics, The Netherlands Cancer Institute, Amsterdam 1066CX, The Netherlands

⁴Department of Hematology, Erasmus University Medical Center, Rotterdam, The Netherlands

⁵Haemato-Oncology Section, The Institute of Cancer Research, Greater London SM5 2NG, UK

⁶These authors contributed equally to this work

*Correspondence: eric.so@kcl.ac.uk

DOI 10.1016/j.stem.2011.05.004

SUMMARY

Bmi1 is required for efficient self-renewal of hematopoietic stem cells (HSCs) and leukemic stem cells (LSCs). In this study, we investigated whether leukemia-associated fusion proteins, which differ in their ability to activate Hox expression, could initiate leukemia in the absence of Bmi1. AML1-ETO and PLZF-RAR α , which do not activate Hox, triggered senescence in Bmi1^{-/-} cells. In contrast, MLL-AF9, which drives expression of Hoxa7 and Hoxa9, readily transformed Bmi1^{-/-} cells. MLL-AF9 could not initiate leukemia in Bmi1^{-/-}Hoxa9^{-/-} mice, which have further compromised HSC functions. But either gene could restore the ability of MLL-AF9 to establish LSCs in the double null background. As reported for Bmi1, Hoxa9 regulates expression of p16^{Ink4a}/p19^{ARF} locus and could overcome senescence induced by AML1-ETO. Together, these results reveal an important functional interplay between MLL/Hox and Bmi1 in regulating cellular senescence for LSC development, suggesting that a synergistic targeting of both molecules is required to eradicate a broader spectrum of LSCs.

INTRODUCTION

Self-renewal is an essential feature for the maintenance of both normal and malignant stem cells. Emerging evidence indicates that pathways critical for self-renewal of normal stem cells are frequently hijacked by malignant stem cells to sustain their immortal growth (Reya et al., 2001). A prominent target is the polycomb group (PcG) protein, Bmi1, which has been shown to be required for normal development of hematopoietic stem cells (HSCs), neural stem cells, and mammary epithelial stem cells (Sauvageau and Sauvageau, 2010). Most notably, in spite of the critical role of Bmi1 in the self-renewal of multiple somatic stem

cells, Bmi1^{-/-} mice can survive to adulthood (up to 20 weeks), suggesting the presence of alternate pathways that may partly compensate for the lack of Bmi1. In acute myeloid leukemia (AML) where leukemic stem cells (LSCs) have been functionally defined (Dick, 2008), chimeric transcription factors (CTFs) resulting from chromosomal translocations represent the most common initiating events (Greaves and Wiemels, 2003) for oncogenic conversion of normal cells into preLSCs and subsequently LSCs (Hong et al., 2008; Yeung et al., 2010). Bmi1 is required for self-renewal of LSCs induced by Meis1 and Hoxa9 oncogenes. In contrast to wild-type (WT) bone marrow cells transduced with Meis1 and Hoxa9 that could induce AML in mice upon serial transplantation, Bmi1^{-/-} cells transduced with the same oncoproteins gradually lost their self-renewal ability and failed to induce AML in secondary transplanted mice (Lessard and Sauvageau, 2003). Although this seminal study has led to the discovery of a previously unrecognized function of Bmi1 in the self-renewal of LSCs, overexpression of Meis1 and Hoxa9 has not been identified as being the initiating event in human AML stem cells, which are mostly initiated by specific CTFs with distinctive transcriptional functions and targets (Greaves et al., 2003; Greaves and Wiemels, 2003). It is not clear whether Bmi1 is also required for the function of bona fide leukemia-associated CTFs in AML stem cells or whether there are alternative pathways that can sustain oncogenic self-renewal in the absence of Bmi1. The most prevalent CTFs arise from mutations of the retinoic acid receptor (RAR α), the core-binding factors (either of its two subunits, AML1 or CBF β), and the mixed lineage leukemia protein (MLL). Such CTFs can be functionally classified according to their dominant transcriptional activities into repressive or activating transcription factors (Cheung and So, 2011; Look, 1997; So and Cleary, 2004). Dominant-repressive CTFs, including chimeric RAR α and AML1 oncoproteins, associate with transcriptional corepressors resulting in suppression of downstream target genes. In contrast, dominant-activating CTFs, such as MLL fusion, recruit transcriptional coactivator complexes leading to the constitutive activation of downstream target genes, including Hox genes (Ayton and Cleary, 2003; So et al., 2004).

Hox proteins represent a group of functionally conserved transcription factors involved in the self-renewal of normal and

malignant stem cells. Certain members of the Hox family are preferentially expressed in HSCs and downregulated during differentiation (Sauvageau et al., 1994). Enforced expression of Hoxb4 leads to stem cell expansion and can significantly enhance long-term hematopoietic reconstitution (Antonchuk et al., 2002). Hoxa9 forms a leukemogenic fusion with Nup98 in AML and has also been proposed as one of the crucial targets for MLL leukemia (Liedtke and Cleary, 2009). However, the critical downstream targets of Hox remain elusive and deletion of any single or multiple Hox gene(s) does not lead to any detectable stem cell defects with the exception of Hoxa9. Hoxa9^{-/-} mice maintained a normal number of HSCs but exhibited weaker reconstitution ability in a competitive transplantation assay (Lawrence et al., 2005; So et al., 2004). Together, these results identify Hox family proteins as critical factors in determining the self-renewal property of HSCs in spite of strong functional redundancy among the family. During embryonic development, Hox gene expression is maintained by antagonistic action between trithorax group (TrxG) proteins such as MLL and PcG proteins (Schuettengruber et al., 2007). Mutation of PcG or TrxG proteins results in homeotic transformations associated with aberrant expression of Hox genes. The homeotic defect in MLL-deficient murine embryos can be partially rescued by deletion of Bmi1 (Hanson et al., 1999). However, this transcriptional network may not be operational in the hematopoietic system where the expression of Hox genes, including Hoxb4, in Bmi1^{-/-} HSCs is not altered (Iwama et al., 2004), suggesting that hematopoietic self-renewal pathways mediated by endogenous Hox may not be grossly affected by the absence of Bmi1.

In this study, we discovered that MLL-AF9, which drives high-level expression of multiple Hox genes, could overcome Bmi1-deficiency to establish LSCs. We further demonstrated a functional crosstalk between Hoxa9 and Bmi1 in regulating cellular senescence for the development of normal hematopoietic and leukemic stem cells. Our results strongly suggest that a synergistic targeting of both Bmi1 and Hoxa9 is required for abolition of certain LSCs such as MLL LSCs with alternative senescence suppression pathways.

RESULTS

Differential Bmi1 Requirement for Transformation by Leukemia-Associated Fusion Proteins

To investigate the roles of Bmi1 in acute leukemogenesis, we compared the transformation ability of three common leukemia-associated CTFs: AML1-ETO-9a (AE), PLZF-RAR α (PR), and MLL-AF9 (MAF9) in primary hematopoietic cells derived from the bone marrow of wild-type or Bmi1^{-/-} mice. To include all the cellular targets for establishment of LSCs, we used c-Kit-enriched cells containing both HSCs and progenitors in the study as previously described (Yeung et al., 2010). As expected, all these fusion proteins could competently transform and enhance the replating ability of wild-type primary hematopoietic cells as determined using a retroviral transduction and transformation assay (RTTA), which has been widely employed as an in vitro surrogate assay for self-renewal properties associated with these CTFs (Cheung et al., 2007; Kwok et al., 2006, 2009, 2010; Lavau et al., 1997; So et al., 2003; Yeung et al., 2010; Zeisig et al., 2007; Zeisig and So, 2009) (Figure 1). In

contrast to vector control transduced cells that exhausted their self-renewal potential in the second round of plating, cells transformed by these CTFs can be serially replated (Figure 1A) to form compact CFU-GEMM (colony forming unit—granulocyte, erythrocyte, monocyte, megakaryocyte)-like colonies (Figure 1B) with an immunophenotype (Figure 1C) and morphology (Figure 1D) consistent with immature myeloid precursors. In the absence of Bmi1, AE and PR gave rise to very few second- and no third-round colonies even though transduced cells could yield a similar number of first-round colonies (see Figure S1A available online), suggesting a functional dependence of Bmi1 for extended self-renewal (Figures 1A and 1B), which is also consistent with a recent observation in the RAR α fusion (Boukarabila et al., 2009). In contrast, Bmi1^{-/-} cells transduced with MAF9 could still efficiently form colonies in the third and subsequent rounds of replating (Figure 1A; data not shown) with similar morphology and immunophenotypes (Figures 1B–1D) as the wild-type transformed cells. The expression level of CTFs, the immunophenotypes, and morphology of the cells/colonies were similar between the wild-type and Bmi1^{-/-}-transduced cells (Figures S1B–S1D). To further characterize the in vivo properties of these cells, we serially transplanted them into syngeneic mice to assess their leukemogenic potential. MAF9-transformed cells derived from a Bmi1^{-/-} background were able to induce leukemia in mice, in spite of a slightly reduced penetrance as compared with MAF9-transformed wild-type cells (Figure 1E). More importantly, when the primary leukemic cells from these animals were transplanted into secondary recipients to further assess their long-term self-renewal property, MAF9 Bmi1^{-/-} leukemic cells could efficiently induce leukemia with an even shorter latency (Figure 1E), indicating that Bmi1 is largely dispensable for establishment and self-renewal of LSCs generated by MAF9. Consistently, the bone marrows of transplanted mice were filled with immature myeloid blasts (Figure 1F), which also infiltrated into different organs including the spleen and liver (Figure 1G). Together, these results revealed contrasting dependence on Bmi1 between different CTFs.

AE and PR Trigger p16^{Ink4a}- and p19^{Arf}-Dependent Senescence in the Absence of Bmi1

Functional complementation experiments were then performed to investigate the potential function of Bmi1 on AE/PR-mediated transformation. As expected, AE, PR, or Bmi1 alone could not transform Bmi1^{-/-} hematopoietic cells. Coexpression of Bmi1 restored the transformation ability of AE and PR (Figure 2A; data not shown). Although transduced cells formed a similar number of first-round colonies (Figure S2A) and expressed a similar level of fusion transcripts (Figure S2B), only Bmi1 co-transduced cells could form compact third-round colonies (Figure 2B). In spite of slightly higher expression levels of Mac-1 and c-Kit, they possessed similar immunophenotype (Figure 2C) and cell morphology (Figure 2D) to wild-type cells transformed by AE or PR.

As compared with wild-type cells, Bmi1^{-/-} cells transduced with AE or PR exhibited severe proliferation defects (Figure 2E; Figure S2C) and an increase in noncycling cells (Figure 2F) as determined by a bromodeoxyuridine (BrdU) incorporation assay, suggesting a cell-cycle defect. Because Bmi1 is a well-known negative regulator of the *cdkn2a* locus encoding cell-cycle

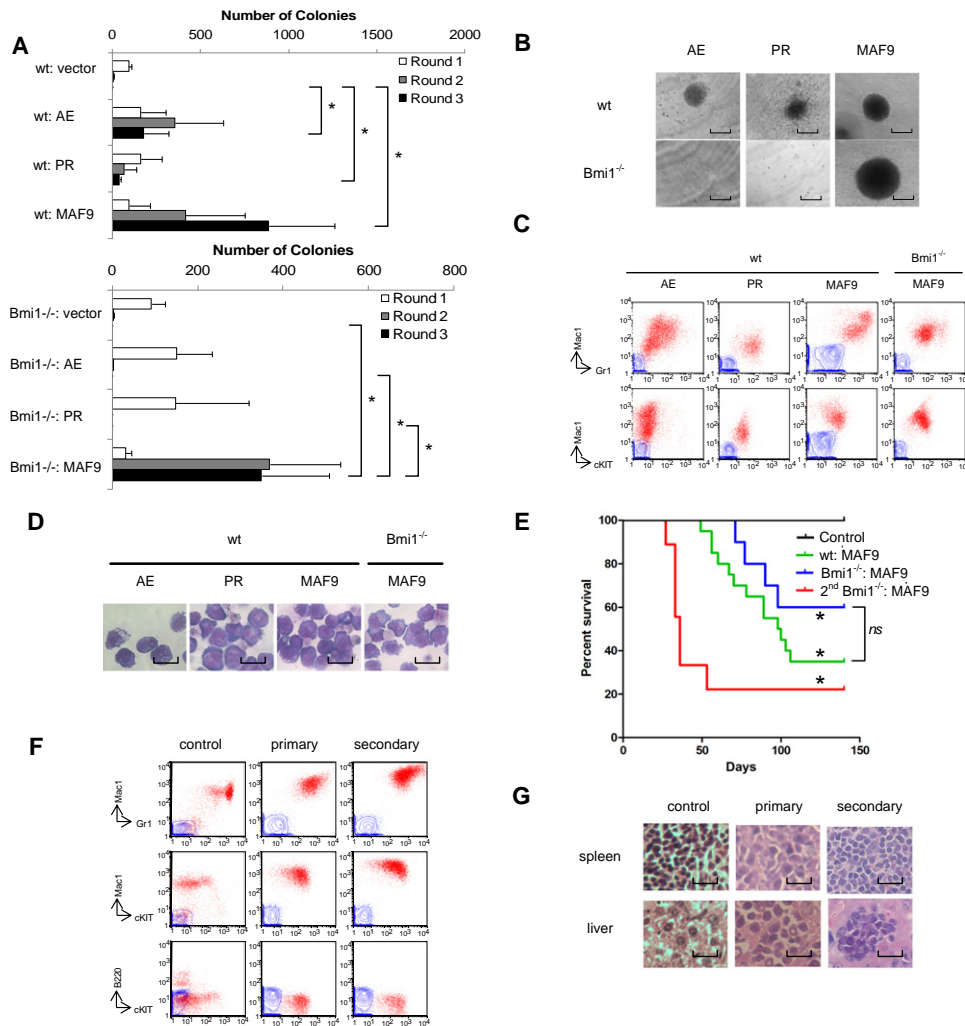


Figure 1. Differential Bmi1-Dependent Transformation by CTFs

(A) Bar charts represent colony numbers in each round of plating in methylcellulose. Error bars represent standard deviation (SD) from at least three independent experiments. AE = AML-ETO9a; PR = PLZF-RAR α ; MAF9 = MLL-AF9.

(B) Typical morphology of third-round colonies from primary BM cells transduced with indicated constructs. Scale bar, 0.2 mm.

(C) Immunophenotype analysis of cells transformed by indicated oncogenes. Dot profiles represent staining obtained with antibodies specific for the indicated cell surface markers. Contour profiles show unstained controls.

(D) Typical cell morphology of primary BM cells transduced with indicated constructs. Scale bar, 10 μ m.

(E) MAF9-transformed Bmi1^{-/-} cells induced leukemia in syngeneic mice, which were transplantable into secondary recipients (wild-type, n = 20; primary Bmi1^{-/-}, n = 10; secondary Bmi1^{-/-}, n = 9; untransduced control, n = 10). *p < 0.05 when comparing the survival curve to the control; ns indicates p > 0.05.

(F) Immunophenotype analysis of leukemic cells recovered from BM of Bmi1^{-/-}: MAF9 injected mice. Dot profiles represent staining obtained with antibodies specific for the indicated cell surface markers. Contour profiles show unstained controls.

(G) Histology of spleen and liver from leukemic mice injected with Bmi1^{-/-}: MAF9. Scale bar, 10 μ m. *p < 0.05 (see also Figure S1).

inhibitors, p16^{Ink4a} and p19^{Arf}, which are linked to cellular senescence, we investigated the effect of these CTFs on their expression in the presence or absence of Bmi1. The absence of Bmi1 resulted in a small but significant change of p16^{Ink4a}/p19^{Arf} expression in c-Kit-enriched hematopoietic cells (Figure 2G; Figure S2D). Similarly, AE or PR elicited a relatively mild increase in p16^{Ink4a} and p19^{Arf} expression in wild-type cells. These were in a stark contrast to the Bmi1^{-/-} cells transduced with AE or PR, which expressed 60- to 300-fold higher levels of p16^{Ink4a} and p19^{Arf} than Bmi1^{-/-} c-Kit cells (Figure 2G). This increase in

p16 expression was also observed at the protein level (Figure 2H). Levels of p16^{Ink4a} and p19^{Arf} (Figure 2G) also showed a strong correlation with proliferation (Figure 2E) and cell-cycle defects (Figure 2F), consistent with the induction of cellular senescence. Conversely, reintroduction of Bmi1 in AE or PR-transduced Bmi1^{-/-} cells suppressed the expression of p16^{Ink4a} and p19^{Arf} (Figure 2G) as well as partly reversed the associated proliferation defects (Figure 2E; Figure S2C) and senescence (Figure 2F). To further confirm the role of Bmi1 in oncogene-induced senescence (OIS), we performed

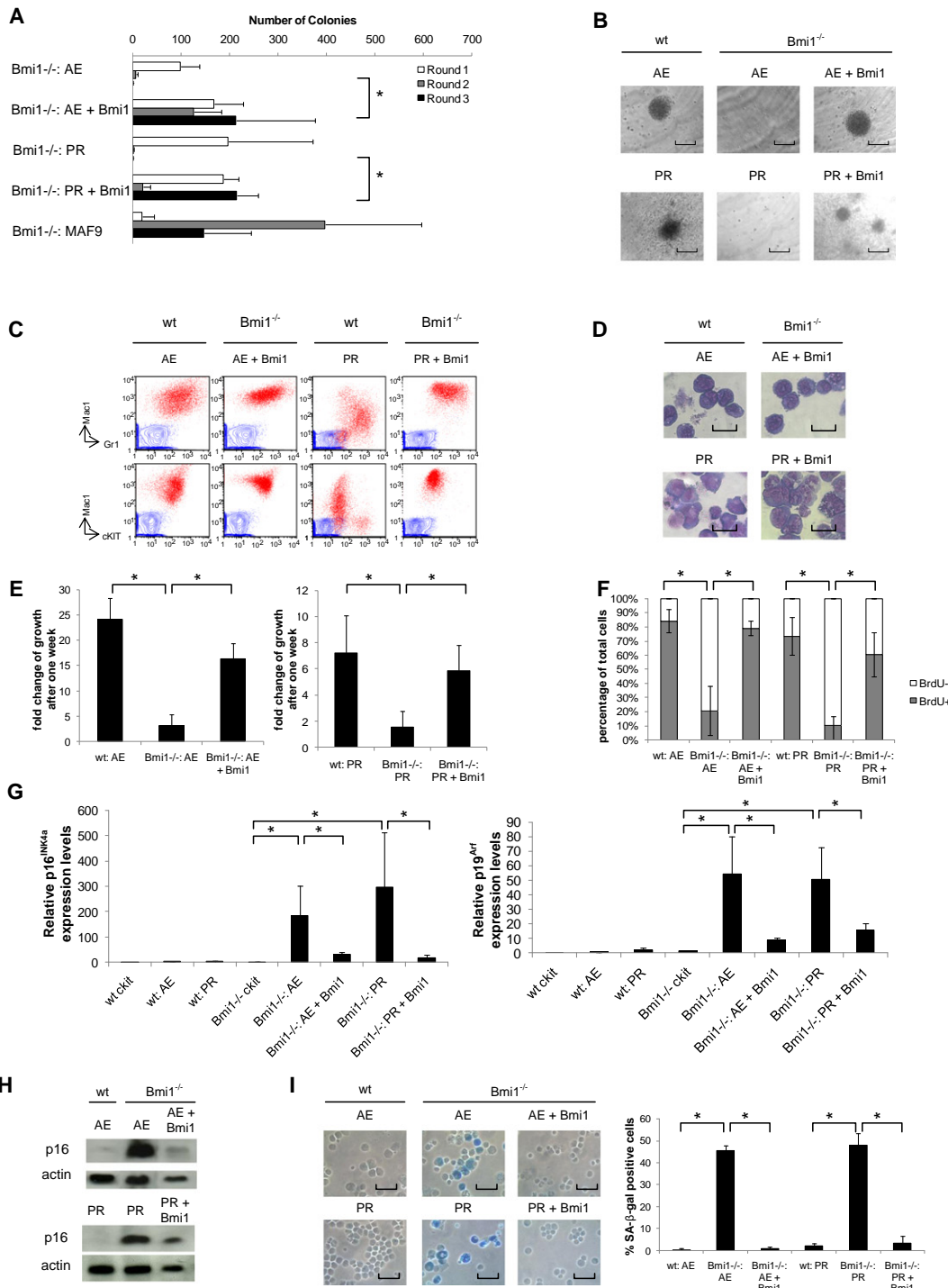


Figure 2. p16/19 Induced Senescence in Bmi1-Dependent Transformation by AE and PR

(A) Bar charts represent colony numbers generated by transduced *Bmi1*^{-/-} cells in each round of plating in methylcellulose for the indicated constructs.

(B) Typical morphology of third-round colonies of primary BM cells transduced with the indicated constructs. Scale bar, 0.2 mm.

(C) Immunophenotype analysis of cells transformed by the indicated constructs. Dot profiles represent staining obtained with antibodies specific for the indicated cell surface markers. Contour profiles show unstained controls.

(D) Typical cell morphology from primary BM cells transduced with indicated constructs. Scale bar, 10 μm.

(E) Bar chart indicates the fold change in cell number after 1 week of growth in OP9 coculture assays for AE (left) and PR (right) transduced cells.

(F) Bar charts show proportion of cycling cells (BrdU⁺) or noncycling cells (BrdU⁻) in AE and PR-transduced *Bmi1*^{-/-} primary BM with or without reintroduction of Bmi1.

(G) *p16*^{INK4a} (left) and *p19*^{ARF} levels (right) after reintroduction of Bmi1 in AE and PR-transduced *Bmi1*^{-/-} cells were expressed relative to the levels in untransduced *Bmi1*^{-/-} c-Kit⁺ cells.

a senescence-associated β -galactosidase (SA- β -gal) assay and annexin V staining in primary hematopoietic cells derived from wild-type and *Bmi1*^{-/-} backgrounds to assess senescence and apoptosis, respectively. We were able to demonstrate a significant induction (in about 45% of the cells) of SA- β -gal activity in *Bmi1*^{-/-} cells transduced with AE or PR, which was suppressed to almost the basal level upon re-expression of *Bmi1* (Figure 2I). In contrast, the level of apoptosis, as determined by annexin V staining, did not reveal a major difference between *Bmi1*^{-/-} cells transduced with CTFs and *Bmi1* rescue (Figure S2E). Together, these results suggest that the requirement for *Bmi1* in leukemogenic transformation by AE and PR could be, in part, explained by its ability to limit OIS induced by these CTFs.

Hoxa9 Is Differentially Activated by MLL Fusions, but Not by AE or PR

To identify the factors that may influence *Bmi1* dependency, we compared the expression profiles of 84 AML patients carrying specific genetic abnormalities including AE (n = 38), RAR α fusions (n = 30 including 26 PML-RAR α and 4 PLZF-RAR α), and MLL fusions (n = 16) (Rice et al., 2009; Valk et al., 2004; Verhaak et al., 2009). Consistent with previous findings on MLL-mediated activation of *HOX* genes reported by others and us (Cheung et al., 2007; Milne et al., 2002; Okada et al., 2005), here we found that a major difference between MLL fusions and AE/RAR α fusions was the significant expression of *HOXA* genes (*HOXA7*, *HOXA9*) and *MEIS1* in MLL leukemia (Figure 3A). Similar results were also observed in our murine models where MAF9, but not AE or PR, fusion-transduced cells expressed high levels of these two *Hox* genes and *Meis1* (Figure 3B). Consistent with the previous findings on *Bmi1*^{-/-} HSCs, the expression of *Hox* genes including *Hoxa9* in CTF-transduced cells were not significantly altered in the absence of *Bmi1* (Figure 3B, left and middle panels, lane 2 and lane 6), suggesting that at least some of these *Hox* genes with alleged self-renewal properties may still function in the absence of *Bmi1*. This is also consistent with the observation that *Bmi1*^{-/-} cells retain limited self-renewal properties that allow *Bmi1*-deficient mice to develop into adulthood. Because both previous overexpression (Bach et al., 2010) and knockout mice studies (Lawrence et al., 2005; So et al., 2004) have demonstrated a dominant function of *Hoxa9* over *Hoxa7* in cellular transformation and maintaining normal HSCs, we generated *Bmi1*^{-/-}*Hoxa9*^{-/-} compound knockout (KO) mice to assess the functional interplay between *Bmi1* and *Hoxa9* in the development of normal hematopoietic and leukemic stem cells.

Hoxa9 Supports Hematopoiesis in the Absence of Bmi1

Although *Bmi1*^{-/-}*Hoxa9*^{-/-} mice were viable, they were sterile and usually died within 6–10 weeks mostly as a result of anemia, compared with *Bmi1*^{-/-} mice with a life span of up to 20 weeks (data not shown). Further analyses of age-matched wild-type and knockout mice revealed that *Bmi1*^{-/-}*Hoxa9*^{-/-} mice had a significant reduction in the cell number in all the hematopoietic

organs analyzed including the bone marrow, spleen, and thymus compared to either *Bmi1*^{-/-} or *Hoxa9*^{-/-} single KO mice (Figures 3C–3E; Figures S3A–S3D), suggesting hematopoietic defects within the HSC and/or early progenitors compartments. Consistently, although knockout of *Hoxa9* alone did not lead to a reduction in the absolute number or percentage of Lin⁻Sca1⁺kit⁺ (LSK) cells (So et al., 2004) (Figure 3F; Tables S1 and S2), *Bmi1*^{-/-}*Hoxa9*^{-/-} mice had a greater than 3-fold reduction in the absolute number of LSK cells in the bone marrow compared with *Bmi1*^{-/-} mice (Figure 3F; Figure S3H; Tables S1 and S2). Using a combination of Flt3 and CD34 as additional markers to further differentiate between long-term HSCs (LT-HSCs), short-term HSCs (ST-HSCs), and multipotent progenitors (MPPs) within the LSK population, we consistently found a significant 3-fold reduction of LT-HSCs in *Bmi1*^{-/-}*Hoxa9*^{-/-} mice as compared with *Bmi1*^{-/-} mice (Figures 3G–3H; Figures S3E–S3J; Tables S1 and S2), suggesting defects originated as early as the LT-HSC stage. Consistent with a stem cell defect, we observed drastic reductions in cell numbers for the downstream myeloid progenitors (Tables S1 and S2) including common myeloid progenitors (CMPs), granulocyte and macrophage progenitors (GMPs), and megakaryocyte and erythrocyte progenitors (MEPs) (Figures 3I–3K; Figures S3K–S3M), whereas its impact on common lymphoid progenitors (CLPs) was relatively mild (Figure 3L; Figure S3N; Tables S1 and S2). In line with the documented roles of *Hoxa9* in T cell development (Lawrence et al., 1997; So et al., 2004), profound defects were found in the thymus of *Bmi1*^{-/-}*Hoxa9*^{-/-} mice. Three out of four subpopulations of pro-T cells (Figures S3O and S3R), CD4/CD8 double-negative (Figure S3S), CD4/CD8 double-positive (Figure S3T), and CD4 or CD8 single-positive T cells (Figures S3U and S3V) were significantly reduced in *Bmi1*^{-/-}*Hoxa9*^{-/-} mice relative to the single KO mice. Further functional assays revealed that *Bmi1*^{-/-}*Hoxa9*^{-/-} bone marrow cells generated reduced numbers of lymphoid and myeloid colonies in vitro (Figure S3W), in which most of latter was more mature CFU-G (Figure S3X). *Bmi1*^{-/-}*Hoxa9*^{-/-} bone marrow cells also failed to achieve long-term repopulation (8+ weeks) although they were able to engraft with compromised ability for short-term reconstitution (4 weeks) (Figures S3Y and S3Z). Together, these results suggest that *Hoxa9* plays a critical role in establishment of HSCs and sustaining normal hematopoiesis in the absence of *Bmi1*.

Deletion of Hoxa9 Completely Abolishes MAF9-Mediated Transformation of Bmi1-Deficient Cells

To further study the function of *Hoxa9* in mediating *Bmi1*-independent transformation, we transduced MAF9 into c-Kit-enriched hematopoietic cells derived from wild-type, *Bmi1*^{-/-}, *Hoxa9*^{-/-}, and *Bmi1*^{-/-}*Hoxa9*^{-/-} mice. As expected, MAF9 could efficiently transform wild-type, *Hoxa9*^{-/-} (Kumar et al., 2004), and *Bmi1*^{-/-} cells, and generated compact third-round colonies with the immunophenotype and morphology consistent of myeloid precursors (Figures 4A–4D). In contrast, although MAF9 could transduce *Bmi1*^{-/-}*Hoxa9*^{-/-} cells to form first-round

(H) Typical immunoblot of p16 in wild-type and *Bmi1*^{-/-} cells transformed with indicated constructs.

(I) Representative SA- β -gal staining of primary BM cells transduced with indicated constructs. Scale bar, 50 μ m. Bar charts indicate the percentage of SA- β -gal-positive cells using the indicated constructs. *p < 0.05. All error bars represent SD from at least three independent experiments (see also Figure S2).

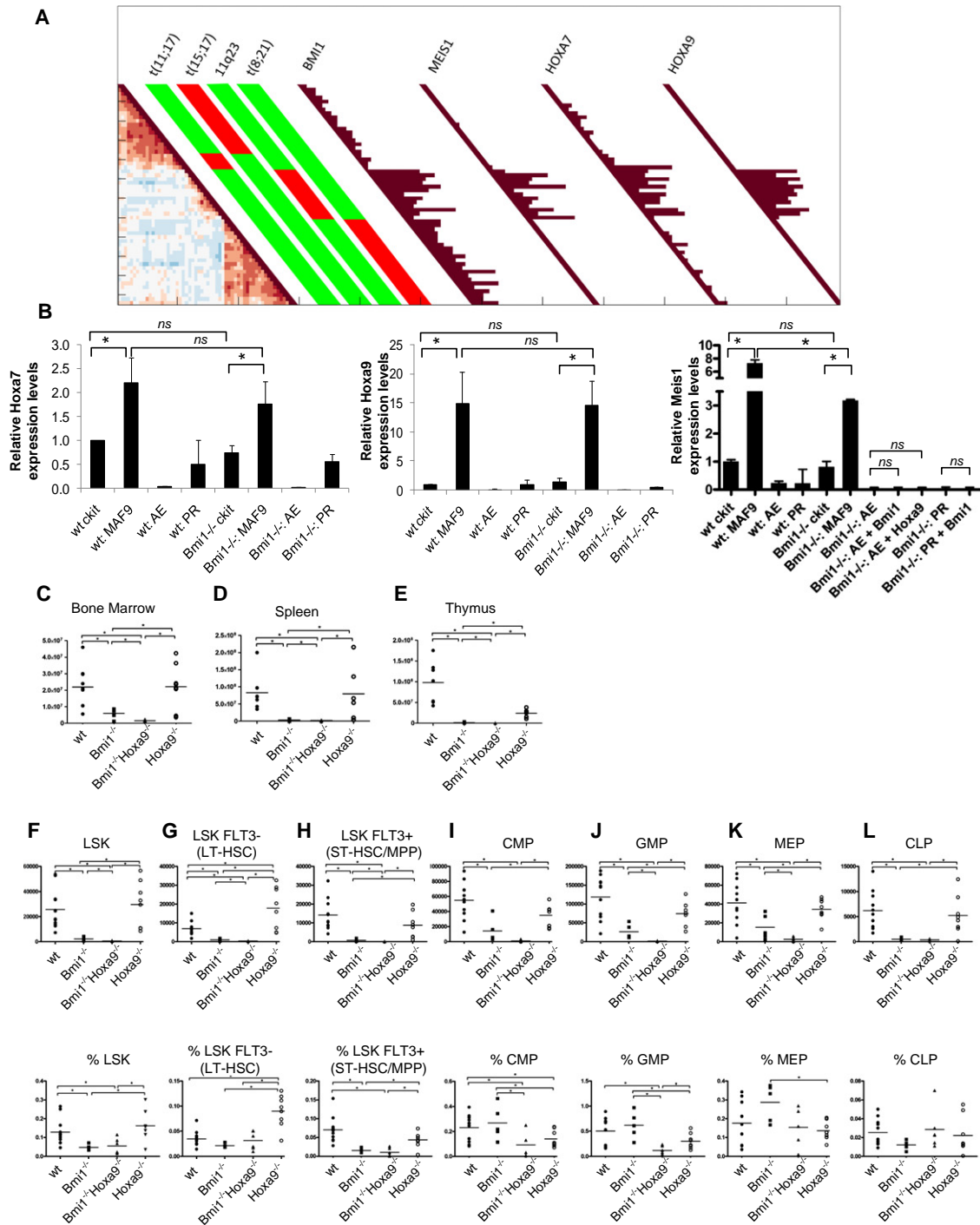


Figure 3. Hox Genes Were Upregulated by MLL Fusions, and Deletion of Hoxa9 Worsened Hematopoietic Defects in *Bmi1*^{-/-} Mice

(A) Pairwise correlations between gene expression profiles of a collection of human AML samples with *MLL*- [11q23], *AML-ETO* [t(8;21)], *PLZF-RARα* [t(11;17)], and *PML-RARα* [t(15;17)] fusions, selected from an original cohort of 530 samples. Colors of the boxes visualize Pearson correlation coefficient: deeper red indicates higher positive correlation; deeper blue indicates higher negative correlation. Green versus red bars: red indicates the cases carrying the indicated translocation. Relative mRNA expression levels of *BMI1*, *MEIS1*, *HOXA7*, and *HOXA9* are indicated in the brown bars next to each patient.

(B–L) (B) Expression of *Hoxa7*, *Hoxa9*, and *Meis1* in wild-type and *Bmi1*^{-/-} primary BM cells and those transduced with the indicated constructs. Expression levels are expressed relative to levels in wild-type c-Kit⁺ cells. Total cell number in the BM (C), spleen (D), and thymus (E) of wild-type (n = 12), *Bmi1*^{-/-} (n = 5), *Bmi1*^{-/-}*Hoxa9*^{-/-} compound KO (n = 6), and *Hoxa9*^{-/-} (n = 8) mice. Each mouse is represented by a symbol; the horizontal line indicates the mean. The absolute number (upper panels) and percentage (lower panels) of LSK (F), LT-HSC (G), ST-HSC/MPP (H), CMP (I), GMP (J), MEP (K), and CLP (L) populations in indicated mice. *p < 0.05; ns indicates p > 0.05 (see also Figure S3 and Tables S1 and S2).

colonies, they quickly exhausted their proliferative potential and failed to produce second- or third-round colonies (Figures 4A–4D), suggesting that Hoxa9 plays a specific role in sustaining MAF9-mediated transformation in the absence of Bmi1.

Functional complementation experiments were performed using *Bmi1*^{-/-}*Hoxa9*^{-/-}-deficient cells transduced with MAF9 in combination with Bmi1 or Hoxa9. All MAF9-transduced cells yielded a similar number of first-round colonies that expressed a similar level of MAF9 transcript (Figures S4A and S4B). Reintroduction of either Bmi1 or Hoxa9 could efficiently rescue the MAF9 transformation phenotype in *Bmi1*^{-/-}*Hoxa9*^{-/-}-deficient cells (Figure 4A). Cotransduced cells produced compact colonies in the third and subsequent rounds of plating with immunophenotype and morphology consistent with myeloid precursors (Figures 4B–4D; data not shown). To further investigate whether re-expression of Hoxa9 could completely rescue the transformation defect of MAF9 in the *Bmi1*^{-/-}*Hoxa9*^{-/-} background, we serially transplanted the Hoxa9 rescued cells into syngeneic mice. As a result, half of the mice transplanted with the *Bmi1*^{-/-}*Hoxa9*^{-/-} cells carrying MAF9 and Hoxa9 developed leukemia within 4 months (Figure 4E). Furthermore, serial transplantation experiments showed that these cells could efficiently transfer leukemia to secondary and even tertiary recipient mice (Figure 4E). Leukemic cells from serial transplants had an immunophenotype consistent with immature myeloid precursors (Figure 4F), which also infiltrated the spleen and, to a much lesser extent, the liver (Figure 4G). Together, these results suggest that Hoxa9 allows establishment and sustains long-term self-renewal of LSCs induced by CTFs in the absence of Bmi1.

Hoxa9 Suppresses Replicative and Oncogene-Induced Senescence

Because an important function of Bmi1 is to suppress the expression of the *cdkn2a* locus, which acts as a major regulator for senescence, and deletion of p16^{Ink4a}/p19^{Arf} can partially rescue the self-renewal defects in *Bmi1*^{-/-}-deficient cells of hematopoietic and neuronal origin (Sauvageau and Sauvageau, 2010), the expression of p16^{Ink4a} and p19^{Arf} was assessed in MAF9-transduced cells. There was a modest induction of p16^{Ink4a} and p19^{Arf} expression by MAF9 in the absence of Bmi1 or Hoxa9 (Figure 4H). However, a significant induction was observed when both Bmi1 and Hoxa9 were inactivated (Figure 4H; Figures S4C and S4D), suggesting a complementary function in regulating these cell-cycle inhibitors. Consistently, expression of Bmi1 or Hoxa9 in cells derived from the double knockout suppressed the induction of p16^{Ink4a} and p19^{Arf} induced by MAF9 (Figure 4H), suggesting a putative function of Hoxa9 in regulating senescence, a critical cellular checkpoint for normal and leukemic stem cells.

To investigate the possible involvement of Hoxa9 in regulating cell senescence, we employed both well-established primary fibroblasts and primary hematopoietic cell models. IMR90 human fibroblasts at a passage close to the onset of senescence were transduced with a vector expressing Hoxa9, an empty vector control, or a vector knocking down p16^{Ink4a} expression. After selection, the proliferative potential of the cells was assessed by colony formation assays. Similar to p16^{Ink4a} knockdown, expression of Hoxa9 conferred a proliferative advantage

to IMR90 cells (Figures 5A and 5B), consistent with a function of Hoxa9 in regulating senescence. To further investigate the role of Hoxa9 in senescence, we took advantage of an inducible system of OIS (Barradas et al., 2009). Primary human fibroblasts carrying inducible Ras oncogene were infected with Hoxa9, a shRNA targeting p16^{Ink4a} or vector control. Upon addition of 4-hydroxytamoxifen (4-OHT) to induce Ras expression, cells transfected with vector control underwent senescence, as observed by reduced incorporation of BrdU and cell growth, characteristic senescent morphology, and induction of p16^{Ink4a} expression (Figures 5C and 5D; data not shown). In contrast, cells infected with a shRNA targeting p16^{Ink4a} or Hoxa9 expression vector partially bypassed OIS and were capable of forming colonies (Figure 5C). When examining the expression of p16^{Ink4a} in these cells, Hoxa9 partially inhibited the induction of p16^{Ink4a} expression observed during OIS (Figure 5D). To further understand how Hoxa9 could control the expression of the *INK4a/ARF* locus, we performed transcription assays using luciferase reporters driven by the p16^{Ink4a} promoter. As expected, ETS2, a known activator of *CDKN2A* locus, (Ohtani et al., 2001) differentially activated reporter gene expression driven by p16^{Ink4a} promoter (Figure 5E). In contrast, Hoxa9 suppressed the basal level of expression of luciferase reporter genes driven by p16^{Ink4a} promoters (Figure 5E). More importantly, coexpression of Hoxa9 significantly suppressed activation of the p16^{Ink4a} promoter by ETS2 (Figure 5E). Interestingly, a putative homeobox binding site has recently been identified in *CDKN2A* locus (Irelan et al., 2009). To determine whether Hoxa9 could indeed bind to this locus, we carried out chromatin immunoprecipitation (ChIP) using IMR90 human fibroblasts or primary murine hematopoietic cells expressing Flag-tagged Hoxa9. A significant enrichment of Hoxa9 binding to the *CDKN2A* locus was detected in both cell types, consistently suggesting the *CDKN2A* locus as a direct transcriptional target of Hoxa9, although further work is required to define the precise binding regions (Figures 5F and 5G; Figure S5A). Because Meis1 is frequently coexpressed with Hox in MLL leukemia (Figures 3A and 3B), we investigated whether Meis1 was also required for the regulation of senescence mediated by Hoxa9. IMR90 primary human fibroblasts were sequentially transfected with either a vector control or Hoxa9, and siRNAs targeting either p16^{Ink4a} (Bishop et al., 2010) or Meis1 (Figure S5B). As expected, expression of Hoxa9 effectively suppressed p16^{Ink4a} levels (Figure S5C). However, in contrast to p16^{Ink4a} siRNA control, sequential knockdown of Meis1 expression by three different shRNAs did not significantly affect the percentage of p16^{Ink4a}-positive cells or BrdU incorporation either in the absence or presence of Hoxa9 (Figures S5D), suggesting that Meis1 may not be directly involved in regulating cell senescence under these conditions. Together, these results reveal a function of Hoxa9 in regulating senescence.

Hoxa9 Rescues AE Oncogene-Induced Senescence in the Absence of Bmi1

Because we previously showed that AE and PR induced senescence in the absence of Bmi1, we sought to determine whether Hoxa9 could also suppress OIS induced by leukemia-associated CTFs in the absence of Bmi1. Analogous to the overexpression of Bmi1 or specific knockdown of p16^{Ink4a} and p19^{Arf} expression

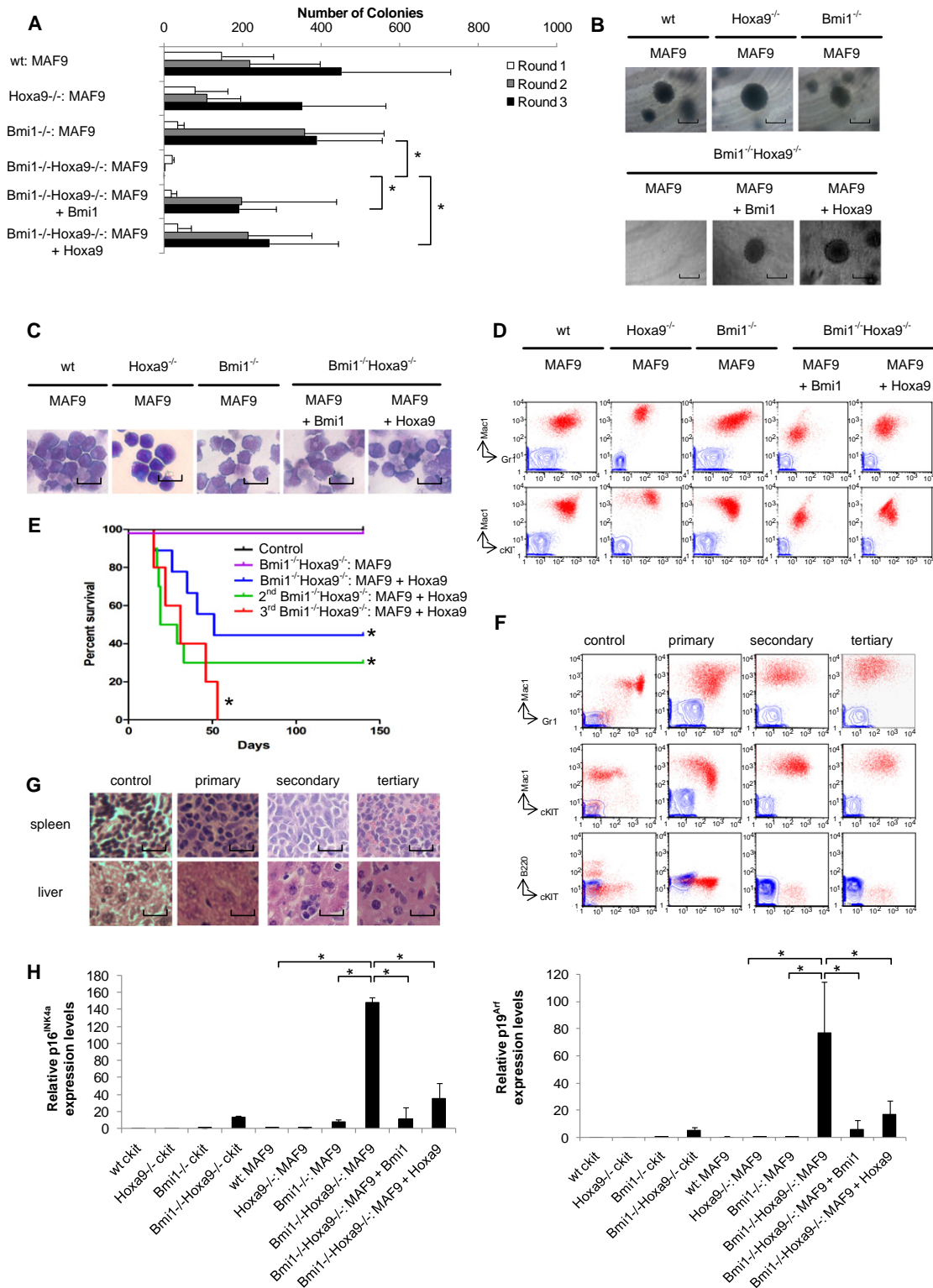


Figure 4. Deletion of Hoxa9 Completely Abolished MLL-AF9-Mediated Transformation of Bmi1-Deficient Cells

(A) Bar chart represents number of colonies in each round of plating in methylcellulose for the indicated constructs.

(B) Typical morphology of third-round colonies of wild-type, *Bmi1*^{-/-}, *Hoxa9*^{-/-}, and *Bmi1*^{-/-}*Hoxa9*^{-/-} cells transformed with indicated constructs. Scale bar, 0.2 mm.

(C) Typical cell morphology of primary BM cells transduced with the indicated constructs after three rounds of plating. Scale bar, 10 μ m.

by a shRNA targeting exon 2 of the *cdkn2a* locus, forced expression of Hoxa9 was able to rescue the Bmi1-dependent transformation mediated by AE (Figure 6A). Although both AE control and AE/Hoxa9 cotransduced cells generated a similar number of first-round colonies (Figure S6A), only the latter formed compact colonies in the third and subsequent rounds of replating with similar morphology (Figure 6B) and immunophenotype (Figure 6C) as the wild-type transformed cells. Coexpression of AE with Hoxa9 in *Bmi1*^{-/-} cells increased the percentage of BrdU-positive cycling cells (Figure 6D), rescued the proliferation defect (Figure 6E), and reduced the percentage of senescent cells (as assessed by SA-β-gal staining in Figure 6F) in AE-transduced *Bmi1*^{-/-} cells to a similar extent as compared with those rescued by Bmi1 overexpression. Hoxa9 also prevented the induction of p16^{Ink4a} and p19^{Arf} expression by AE in *Bmi1*^{-/-} cells (Figures 6G and 6H), consistently supporting the role of Hoxa9 in regulating OIS for development of LSCs.

DISCUSSION

Although Bmi1 has previously been shown to be an essential molecule required for LSCs induced by overexpression of Meis1 and Hoxa9, we illustrate that the requirement of Bmi1 for the establishment of AML stem cells differs vastly depending on the nature of the initiating events. As a result of gene fusion, CTFs acquire aberrant transcriptional and epigenetic properties that can initiate novel and distinctive transcriptional programs to convert early progenitors/stem cells into preLSCs and subsequently LSCs (Greaves and Wiemels, 2003; Hong et al., 2008; Yeung et al., 2010). In contrast to AML1 and RAR α fusions that act as dominant transcriptional repressors, MLL fusions aberrantly recruit transcriptional activators such as Dot1L (Okada et al., 2005) and Prmt1 (Cheung et al., 2007) to mediate epigenetic reprogramming to induce stem cell-like transcriptional programs including activation of multiple *Hox* genes (Krivtsov et al., 2006, 2008; So et al., 2004; Zeisig et al., 2008). Interestingly, *Hox* genes have also been suggested as downstream targets of RAR α and AML1-fusions (Look, 1997), which may increase the Bmi1-dependence of these fusions for suppression of OIS. Thus, the proposed function of the *Hox* gene in suppressing cellular senescence may constitute a critical determinant for Bmi1-independent establishment and maintenance of LSCs by different CTFs (Figure 7).

In comparison to Meis1/Hoxa9 oncogenes, MLL fusions acting directly upstream of these two proteins can activate an even larger array of transcriptional programs including multiple *Hox* genes and non*Hox* targets. Although it is evident that over-

expression of a single *Hox* gene is not sufficient to fully rescue the self-renewal defect associated with loss of Bmi1, forced expression of Hoxb4 alone can lead to expansion of short-term repopulating HSCs in the absence of Bmi1 (Faubert et al., 2008) in spite of a lack of long-term reconstitution potential (Iwama et al., 2004). Similarly, *Bmi1*^{-/-} cells transformed by Hoxa9/Meis1 can still induce malignant myeloid expansion and acute leukemia in primary transplanted mice (Lessard and Sauvageau, 2003). The finding that MLL CTFs acting as a master *Hox* activator can overcome Bmi1 dependency supports the notion that synergistic activation of multiple *Hox* genes may allow Bmi1-independent self-renewal. However, given the absolute Bmi1-dependent self-renewal of LSCs induced by Meis1/Hoxa9, other non*Hox* MLL targets may also cooperate with *Hox* in the process of the Bmi1-independent transformation. MLL fusions have been shown to directly regulate expression of cell-cycle inhibitors such as p27^{Kip1} (Liu et al., 2009). Although further studies dissecting the multifaceted transcriptional functions of MLL fusions will be needed to identify novel candidates accounting for the Bmi1 independence, the current results clearly indicate that Bmi1 requirement is oncogene dependent and that therapeutic targeting of Bmi1 alone may not be sufficient for eradication of certain cancer stem cells.

Although *Hox* genes have been implicated in the self-renewal of HSCs, a complete knockout of any single or multiple *Hox* gene(s), including *Hoxa9*, has no or very modest effects on HSC development (Bijl et al., 2006; Björnsson et al., 2003; Brun et al., 2004; Lawrence et al., 2005; So et al., 2004), suggesting the presence of non*Hox* complementary pathways. Although *Hoxa9* is largely dispensable for establishment of normal HSCs in the wild-type background (So et al., 2003), it plays a critical role in the generation of HSCs and for maintaining normal hematopoiesis in the absence of Bmi1. Similarly, whereas *Hoxa9* is normally dispensable for transformation mediated by a number of MLL fusions including MAF9 and MLL-GAS7 (Kumar et al., 2004; So et al., 2004), it becomes essential for the establishment of MAF9 LSCs in the absence of Bmi1, revealing a critical functional interplay between these two molecular pathways in establishment of normal and leukemic stem cells. In contrast to the PcG protein, CBX7, whose overexpression partially prevents Bmi1-dependent senescence by a mechanism reliant on PRCs function (Gil et al., 2004), *Hoxa9* has not been reported to be part of the PRCs. Although *Hoxa9* may have multiple functions, its direct binding and transcriptional repression of the *CDKN2A* locus suggest that *Hoxa9* may partially replace Bmi1 function by suppressing cellular senescence, although the precise interplay between *Hoxa9* and PRCs remains to be established.

(D) Immunophenotype analysis of cells transformed by indicated constructs. Contour profiles represent staining obtained with antibodies specific for the indicated cell surface markers. Dot profiles show unstained controls.

(E) Mice injected with *Bmi1*^{-/-}*Hoxa9*^{-/-} compound KO cells transduced with MAF9 and Hoxa9 develop myeloid leukemia (n = 9), which were serially transplantable into secondary (second, n = 10) and tertiary mice (third, n = 5). Direct injection of *Bmi1*^{-/-}*Hoxa9*^{-/-} cells transformed with MAF9 (n = 8) did not result in leukemia (control, n = 10). *p < 0.05 when comparing the survival curve to the control.

(F) Immunophenotype analysis of leukemic cells recovered from BM of injected mice. Dot profiles represent staining obtained with antibodies specific for the indicated cell surface markers. Contour profiles show unstained controls.

(G) Histology of spleen and liver from leukemic mice injected with *Bmi1*^{-/-}*Hoxa9*^{-/-}: MAF9 + Hoxa9 cells. Scale bar, 10 μ m.

(H) p16^{Ink4a} (left) and p19^{Arf} (right) expression levels in primary hematopoietic cells derived from different KO or wild-type backgrounds transduced with indicated constructs. Values were expressed relative to levels in *Bmi1*^{-/-} c-Kit⁺ cells. *p < 0.05. All error bars represent SD from at least three independent experiments (see also Figure S4).

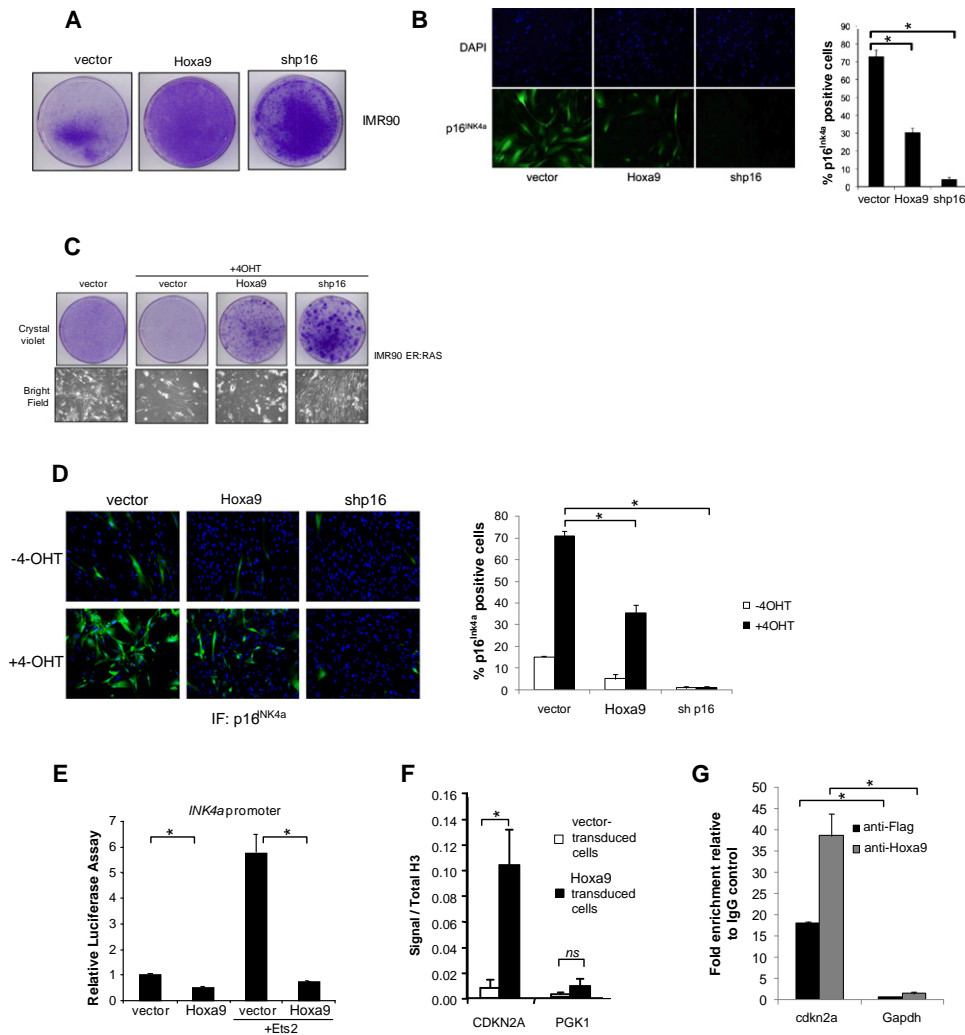


Figure 5. Hoxa9 Suppressed Replicative and Oncogene-Induced Senescence

(A) IMR90 primary human fibroblasts transfected with the indicated vectors were fixed and stained with crystal violet after 10–15 days.
 (B) Immunophenotype of p16 in IMR90 cells overexpressing indicated constructs. Right-hand chart indicates percentage of p16^{INK4a}-positive cells observed. *p < 0.05.
 (C) IMR90 ER:Ras cells were transfected with vector control, Hoxa9, or a shRNA targeting human p16^{INK4a}. Top row shows crystal violet stained cells, lower shows bright field images.
 (D) Immunofluorescence staining of p16^{INK4a} in IMR90 ER:Ras human fibroblast 4 days after 4-OHT induction. Right-hand chart indicates percentage of p16^{INK4a}-positive cells observed.
 (E) Luciferase assay with p16^{INK4a} promoter-driven reporter.
 (F) Bar charts show the relative binding of Hoxa9 (by Flag-antibody) to *CDKN2A* or *PGK1* loci in human fibroblasts expressing Flag-tagged Hoxa9 or vector control.
 (G) Bar charts show the relative binding of Hoxa9 (by Flag-antibody or Hoxa9 antibody) to *cdkn2a* or *gapdh* loci in primary murine hematopoietic cells expressing Flag-tagged Hoxa9. *p < 0.05; ns indicates p > 0.05. All error bars represent SD from at least three independent experiments (see also Figure S5).

Interestingly, HOXA9 has been identified as one of the most significant independent poor prognostic markers for AML, but very little is known about its functions and critical downstream targets (Golub et al., 1999). The newly discovered functional interplay of Hoxa9 with Bmi1 in development of normal and leukemic stem cells will provide a potential molecular explanation for its role in influencing AML prognosis. Hoxa9 can regulate *Ink4a/Arf* expression and cellular senescence in the presence (Figure 5) or absence of Bmi1 (Figure 6). In this model, we

propose that both Bmi1 and Hox can function to suppress cellular senescence, whereby one of the pathways is needed to overcome OIS by certain CTFs (Figure 7). In contrast to AE and PR, which are critically dependent on Bmi1 for their transformation, MLL CTFs that are capable of activating multiple *Hox* targets can bypass Bmi1 requirement. These findings reveal an unexpected cooperative function between Bmi1 and MLL/Hox, and that a synergistic targeting of both molecules may be required for elimination of certain cancer stem cells (Figure 7).

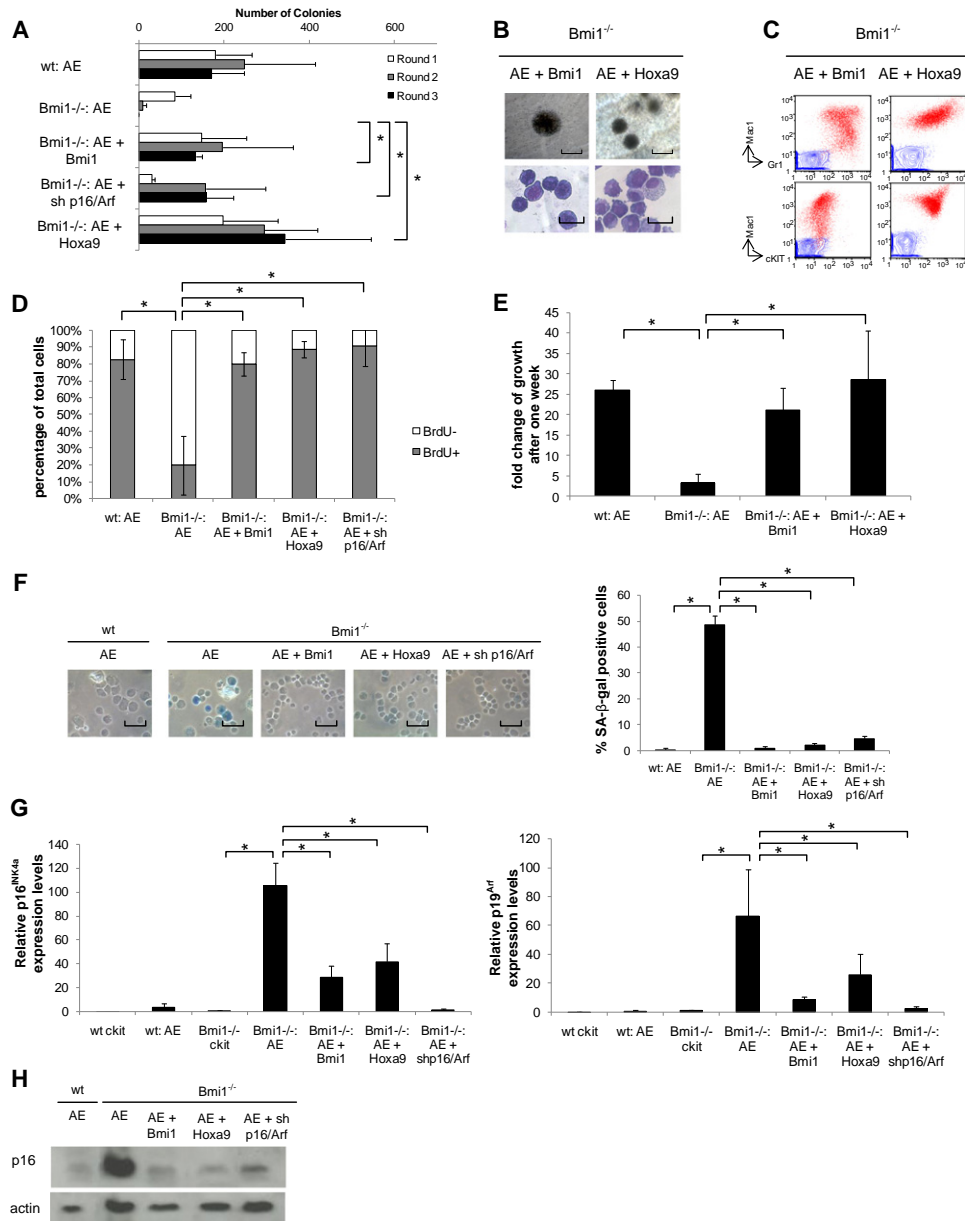


Figure 6. Hoxa9 Rescued Oncogene-Induced Senescence by AE in the Absence of Bmi1

(A) Bar charts represent colony number in each round of plating in methylcellulose.
 (B) Typical morphology of third-round colonies (top; scale bar, 0.2 mm) and cell morphology (bottom; scale bar, 10 μm) from *Bmi1*^{-/-} primary BM cells transduced with the indicated constructs.
 (C) Immunophenotype analysis of cells transformed by the indicated constructs. Dot profiles represent staining obtained with antibodies specific for the indicated cell surface markers. Contour profiles show unstained controls.
 (D) Bar charts show proportion of cycling cells (BrdU⁺) or noncycling cells (BrdU⁻) in AE-transformed WT or *Bmi1*^{-/-} primary BM with or without reintroduction of Bmi1, Hoxa9, or shp16/ARF.
 (E) The bar chart indicates the fold change in cell number after 1 week in OP9 coculture assays.
 (F) Typical SA-β-gal staining of primary BM cells transduced with indicated constructs. Scale bar, 50 μm. Bar charts indicate the percentage of SA-β-gal-positive cells induced by the indicated constructs.
 (G) *p16*^{INK4a} (left) and *p19*^{ARF} (right) expression levels expressed relative to levels in *Bmi1*^{-/-} c-Kit⁺ cells. **p* < 0.05. All error bars represent SD from at least three independent experiments.
 (H) Typical immunoblot of p16 in wild-type and *Bmi1*^{-/-} cells transduced with indicated constructs (see also Figure S6).

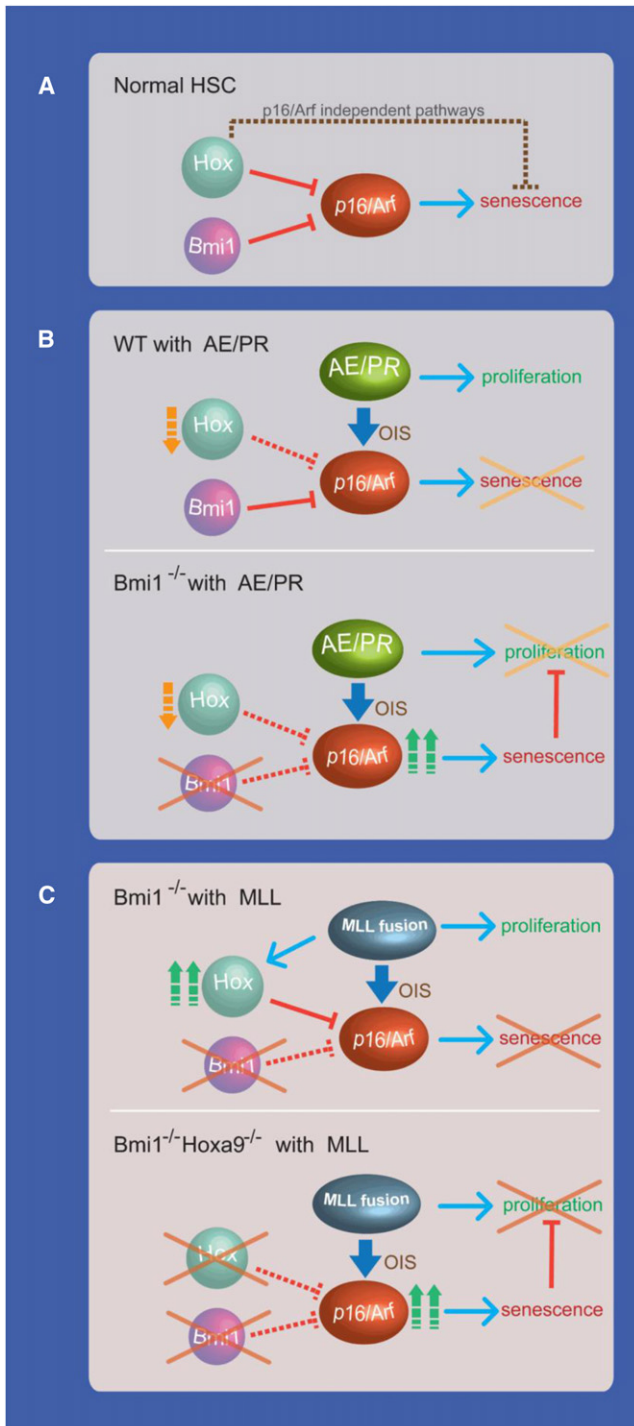


Figure 7. Bmi1 and Hox Can Function to Suppress Cellular Senescence

(A–C) (A) Bmi1 and Hox proteins may function to suppress expression of the *Ink4a/Arf* locus to preserve HSCs pool. In the context of leukemia, formation of an oncogenic fusion protein confers proliferative advantage but also induces OIS of the targeted hematopoietic cells. Depending on the nature of these initiating events and the origin of the targeted cells (e.g., stem cells versus progenitors), certain oncoproteins, such as AE/PR, are completely dependent on Bmi1 to suppress OIS (B). Other oncogenes, such as MLL fusions, which can activate multiple Hox genes, exhibit a modest dependence on Bmi1

EXPERIMENTAL PROCEDURES

Constructs

MSCV retroviral plasmids encoding full-length AE, PR, and MLL-AF9 cDNA have been previously described (Cheung et al., 2007; Kwok et al., 2006, 2009; Wong et al., 2007).

Retroviral Transduction Transplantation Assay

Retroviral Transduction Transplantation Assay (RTTA) was performed as previously described (Zeisig and So, 2009). Briefly, c-Kit⁺ cells were isolated from murine bone marrow (BM) using CD117 MicroBeads (Miltenyi Biotech) and were cultured overnight in R10 medium (see Supplemental Information) supplemented with 20 ng ml⁻¹ stem cell factor (SCF), 10 ng ml⁻¹ interleukin (IL)-3, and 10 ng ml⁻¹ IL-6. 4 × 10⁴ Bmi1^{-/-} or Bmi1^{-/-}Hoxa9^{-/-} or 2 × 10⁴ WT c-Kit⁺ cells were transduced for each test condition. Concentrated viral supernatant was used for transduction by centrifugation at 800 × g in the presence of 5 μg ml⁻¹ polybrene (Sigma-Aldrich) at 32°C for 2 hr. A second transduction was performed on the following day. Cells were subsequently plated into 1% methylcellulose medium (M3231; Stem Cell Technologies) containing 20 ng ml⁻¹ SCF, 10 ng ml⁻¹ IL-3, 10 ng ml⁻¹ IL-6, and 10 ng ml⁻¹ granulocyte macrophage colony-stimulating factor (GM-CSF) and appropriate selection antibiotic. Colonies were scored after 7 days of culture and replated every 7 days. After the third or fourth round of plating, cells were cultured in R20/20 (see Supplemental Information) to establish cell lines. All recombinant murine cytokines were purchased from PeprotechEC.

Immunophenotype Analysis

Immunophenotype analysis of cells was performed by flow cytometry as previously described (Cheung et al., 2007; Kwok et al., 2006) and detailed in the Supplemental Experimental Procedures. Immunophenotype analysis of hematopoietic compartments in the knockout mice was performed as described (So et al., 2004; Yeung and So, 2009) and detailed in the Supplemental Experimental Procedures.

Proliferation Coculture and Cycling Assays

Cells from the RTTA assays were used in OP9 coculture and BrdU incorporation assays. BrdU incorporation was determined by flow cytometry using FITC BrdU Flow Kit (BD Biosciences) following manufacturer's instructions after incubating cells for 20 hr with BrdU. Details of cell culture are provided in the Supplemental Experimental Procedures. For coculture studies, OP9 cells were irradiated at 30 Gy and plated at a density of approximately 1 × 10⁴ cells/cm² in 12-well plates. 4 × 10⁵ hematopoietic cells were seeded on the following day and were counted after a week of growth before 2 × 10⁵ cells were plated into methylcellulose for clonogenic formation assay as described in RTTA.

Experimental Animals and In Vivo Assays

Bmi1^{+/-} mice (van der Lugt et al., 1994) were crossed with Hoxa9^{-/-} mice (So et al., 2004) to obtain Bmi1^{+/-}Hoxa9^{-/-} mice and, subsequently, Bmi1^{-/-}Hoxa9^{-/-} compound KO mice. For transplantation experiments to determine leukemogenicity of test cells, C57BL/6 or SJL mice were given 12.5 Gy total body γ-irradiation and injected intravenously with 1 × 10⁶ test cells mixed with 0.2 × 10⁶ C57BL/6 or SJL mononuclear BM cells. Control mice were injected with 0.2 × 10⁶ C57BL/6 or SJL mononuclear BM cells. All experimental procedures were approved by the King's College London and Institute of Cancer Research animal welfare and ethics committees and conformed to the UK Home Office regulations.

Senescence-Associated β-galactosidase Staining

Cytospins of cells from RTTAs were fixed with 0.5% glutaraldehyde (w/v) for 15 min and then washed twice with 1 mM MgCl₂ in PBS (pH 6.0). X-Gal staining solution (1 mg ml⁻¹ X-Gal, 5 mM K₃[Fe(CN)₆], and 5 mM K₄[Fe(CN)₆] in 1 mM MgCl₂/PBS (pH 6.0)) was added to the cells for 2–24 hr, after which the cells

function (C). For the latter, synergistic targeting of both Bmi1 and Hox pathways may be required to eradicate LSCs.

were washed with water. Pictures of cytopspins were taken using a Wolfe XD-202 microscope with a GXCAM-3 camera using GXCapture software (GX Optical). The percentage of SA- β -gal-positive cells was determined upon counting of at least 200 cells.

Chromatin Immunoprecipitation

ChIP was performed as previously described (Ananthanarayanan et al., 2004) with minor modifications using the EZ-Magna ChIP™ G kit (cat no. 17-409, Millipore). Immunoprecipitation of crosslinked chromatin was conducted with anti-FLAG mouse monoclonal magnetic beads (Sigma-Aldrich cat no. M8823-5). After immunoprecipitation, DNA was extracted using the QIAquick PCR purification kit (QIAGEN) and an aliquot amplified by real time qPCR using oligonucleotide primers described in the Supplemental Experimental Procedures. To confirm target enrichment, we evaluated each PCR product first by standard endpoint PCR. ChIP on primary murine cell lines was performed as previously described (Barradas et al., 2009; Cheung et al., 2007).

Detailed procedures for cell culture, immunophenotype analysis, annexin V staining, immunofluorescence staining, crystal violet staining, qPCR, western blotting, luciferase reporter assay, and statistical analysis are in the Supplemental Information.

SUPPLEMENTAL INFORMATION

Supplemental Information includes six figures, two tables, and Supplemental Experimental Procedures and can be found with this article online at doi:10.1016/j.stem.2011.05.004.

ACKNOWLEDGMENTS

We thank M. Cleary for his help and constructive advice in the early phase of the project in particular; M. Greaves for critical discussion; J. Licht and K. Rice for providing clinical data and bioinformatic support on the t(11; 17) cases; N. Cheung, E. Amin, W. Vetharoy, C. Kwok, A. Thornhill, C. Foley, I. Tittley, and G. Vijayaraghavan for technical assistance; D.E. Zhang, R. Slany, and C.V. Dang for provision of useful reagents; G. Dickson, A. Thompson, and T. Lappin for initial help in Hox qPCR analysis; and P. Tse for professional graphic assistance. J.G. and N.P. are funded by the MRC. C.-W.-E.S. is an AICR fellow and EMBO young investigator. This work is supported by CRUK and in part by LLR.

Received: March 10, 2010

Revised: January 7, 2011

Accepted: May 6, 2011

Published: June 2, 2011

REFERENCES

Ananthanarayanan, M., Li, S., Balasubramanian, N., Suchy, F.J., and Walsh, M.J. (2004). Ligand-dependent activation of the farnesoid X-receptor directs arginine methylation of histone H3 by CARM1. *J. Biol. Chem.* 279, 54348–54357.

Antonchuk, J., Sauvageau, G., and Humphries, R.K. (2002). HOXB4-induced expansion of adult hematopoietic stem cells ex vivo. *Cell* 109, 39–45.

Ayton, P.M., and Cleary, M.L. (2003). Transformation of myeloid progenitors by MLL oncoproteins is dependent on Hoxa7 and Hoxa9. *Genes Dev.* 17, 2298–2307.

Bach, C., Buhl, S., Mueller, D., García-Cuellar, M.P., Maethner, E., and Slany, R.K. (2010). Leukemogenic transformation by HOXA cluster genes. *Blood* 115, 2910–2918.

Barradas, M., Anderton, E., Acosta, J.C., Li, S., Banito, A., Rodriguez-Niedenführ, M., Maertens, G., Banck, M., Zhou, M.M., Walsh, M.J., et al. (2009). Histone demethylase JMJD3 contributes to epigenetic control of INK4a/ARF by oncogenic RAS. *Genes Dev.* 23, 1177–1182.

Bijl, J., Thompson, A., Ramirez-Solis, R., Kros, J., Grier, D.G., Lawrence, H.J., and Sauvageau, G. (2006). Analysis of HSC activity and compensatory Hox gene expression profile in Hoxb cluster mutant fetal liver cells. *Blood* 108, 116–122.

Bishop, C.L., Bergin, A.M., Fessart, D., Borgdorff, V., Hatzimasoura, E., Garbe, J.C., Stampfer, M.R., Koh, J., and Beach, D.H. (2010). Primary cilium-dependent and -independent Hedgehog signaling inhibits p16(INK4A). *Mol. Cell* 40, 533–547.

Björnsson, J.M., Larsson, N., Brun, A.C., Magnusson, M., Andersson, E., Lundström, P., Larsson, J., Repetowska, E., Ehinger, M., Humphries, R.K., and Karlsson, S. (2003). Reduced proliferative capacity of hematopoietic stem cells deficient in Hoxb3 and Hoxb4. *Mol. Cell. Biol.* 23, 3872–3883.

Boukarabila, H., Saurin, A.J., Batsché, E., Mossadegh, N., van Lohuizen, M., Otte, A.P., Pradel, J., Muchardt, C., Sieweke, M., and Duprez, E. (2009). The PRC1 Polycomb group complex interacts with PLZF/RARA to mediate leukemic transformation. *Genes Dev.* 23, 1195–1206.

Brun, A.C., Björnsson, J.M., Magnusson, M., Larsson, N., Leveén, P., Ehinger, M., Nilsson, E., and Karlsson, S. (2004). Hoxb4-deficient mice undergo normal hematopoietic development but exhibit a mild proliferation defect in hematopoietic stem cells. *Blood* 103, 4126–4133.

Cheung, N., and So, C.W. (2011). Transcriptional and epigenetic networks in haematological malignancy. *FEBS Lett.* in press. Published online April 6, 2011. 10.1016/j.febslet.2011.03.068.

Cheung, N., Chan, L.C., Thompson, A., Cleary, M.L., and So, C.W. (2007). Protein arginine-methyltransferase-dependent oncogenesis. *Nat. Cell Biol.* 9, 1208–1215.

Dick, J.E. (2008). Stem cell concepts renew cancer research. *Blood* 112, 4793–4807.

Faubert, A., Chagraoui, J., Mayotte, N., Fréchette, M., Iscove, N.N., Humphries, R.K., and Sauvageau, G. (2008). Complementary and independent function for Hoxb4 and Bmi1 in HSC activity. *Cold Spring Harb. Symp. Quant. Biol.* 73, 555–564.

Gil, J., Bernard, D., Martínez, D., and Beach, D. (2004). Polycomb CBX7 has a unifying role in cellular lifespan. *Nat. Cell Biol.* 6, 67–72.

Golub, T.R., Slonim, D.K., Tamayo, P., Huard, C., Gaasenbeek, M., Mesirov, J.P., Collier, H., Loh, M.L., Downing, J.R., Caligiuri, M.A., et al. (1999). Molecular classification of cancer: class discovery and class prediction by gene expression monitoring. *Science* 286, 531–537.

Greaves, M.F., and Wiemels, J. (2003). Origins of chromosome translocations in childhood leukaemia. *Nat. Rev. Cancer* 3, 639–649.

Greaves, M.F., Maia, A.T., Wiemels, J.L., and Ford, A.M. (2003). Leukemia in twins: lessons in natural history. *Blood* 102, 2321–2333.

Hanson, R.D., Hess, J.L., Yu, B.D., Ernst, P., van Lohuizen, M., Berns, A., van der Lugt, N.M., Shashikant, C.S., Ruddle, F.H., Seto, M., and Korsmeyer, S.J. (1999). Mammalian Trithorax and polycomb-group homologues are antagonistic regulators of homeotic development. *Proc. Natl. Acad. Sci. USA* 96, 14372–14377.

Hong, D., Gupta, R., Ancliff, P., Atzberger, A., Brown, J., Soneji, S., Green, J., Colman, S., Piacibello, W., Buckle, V., et al. (2008). Initiating and cancer-propagating cells in TEL-AML1-associated childhood leukemia. *Science* 319, 336–339.

Irelan, J.T., Gutierrez Del Arroyo, A., Gutierrez, A., Peters, G., Quon, K.C., Miraglia, L., and Chanda, S.K. (2009). A functional screen for regulators of CKDN2A reveals MEOX2 as a transcriptional activator of INK4a. *PLoS ONE* 4, e5067.

Iwama, A., Oguro, H., Negishi, M., Kato, Y., Morita, Y., Tsukui, H., Ema, H., Kamijo, T., Katoh-Fukui, Y., Koseki, H., et al. (2004). Enhanced self-renewal of hematopoietic stem cells mediated by the polycomb gene product Bmi-1. *Immunity* 21, 843–851.

Krivtsov, A.V., Twomey, D., Feng, Z., Stubbs, M.C., Wang, Y., Faber, J., Levine, J.E., Wang, J., Hahn, W.C., Gilliland, D.G., et al. (2006). Transformation from committed progenitor to leukaemia stem cell initiated by MLL-AF9. *Nature* 442, 818–822.

Krivtsov, A.V., Feng, Z., Lemieux, M.E., Faber, J., Vempati, S., Sinha, A.U., Xia, X., Jesneck, J., Bracken, A.P., Silverman, L.B., et al. (2008). H3K79 methylation profiles define murine and human MLL-AF4 leukemias. *Cancer Cell* 14, 355–368.

- Kumar, A.R., Hudson, W.A., Chen, W., Nishiuchi, R., Yao, Q., and Kersey, J.H. (2004). Hoxa9 influences the phenotype but not the incidence of MLL-AF9 fusion gene leukemia. *Blood* 103, 1823–1828.
- Kwok, C., Zeisig, B.B., Dong, S., and So, C.W. (2006). Forced homo-oligomerization of RARalpha leads to transformation of primary hematopoietic cells. *Cancer Cell* 9, 95–108.
- Kwok, C., Zeisig, B.B., Qiu, J., Dong, S., and So, C.W. (2009). Transforming activity of AML1-ETO is independent of CBFbeta and ETO interaction but requires formation of homo-oligomeric complexes. *Proc. Natl. Acad. Sci. USA* 106, 2853–2858.
- Kwok, C., Zeisig, B.B., Dong, S., and So, C.W. (2010). The role of CBFbeta in AML1-ETO's activity. *Blood* 115, 3176–3177.
- Lavau, C., Szilvassy, S.J., Slany, R., and Cleary, M.L. (1997). Immortalization and leukemic transformation of a myelomonocytic precursor by retrovirally transduced HRX-ENL. *EMBO J.* 16, 4226–4237.
- Lawrence, H.J., Helgason, C.D., Sauvageau, G., Fong, S., Izon, D.J., Humphries, R.K., and Largman, C. (1997). Mice bearing a targeted interruption of the homeobox gene HOXA9 have defects in myeloid, erythroid, and lymphoid hematopoiesis. *Blood* 89, 1922–1930.
- Lawrence, H.J., Christensen, J., Fong, S., Hu, Y.L., Weissman, I., Sauvageau, G., Humphries, R.K., and Largman, C. (2005). Loss of expression of the Hoxa-9 homeobox gene impairs the proliferation and repopulating ability of hematopoietic stem cells. *Blood* 106, 3988–3994.
- Lessard, J., and Sauvageau, G. (2003). Bmi-1 determines the proliferative capacity of normal and leukaemic stem cells. *Nature* 423, 255–260.
- Liedtke, M., and Cleary, M.L. (2009). Therapeutic targeting of MLL. *Blood* 113, 6061–6068.
- Liu, H., Cheng, E.H., and Hsieh, J.J. (2009). MLL fusions: pathways to leukemia. *Cancer Biol. Ther.* 8, 1204–1211.
- Look, A.T. (1997). Oncogenic transcription factors in the human acute leukemias. *Science* 278, 1059–1064.
- Milne, T.A., Briggs, S.D., Brock, H.W., Martin, M.E., Gibbs, D., Allis, C.D., and Hess, J.L. (2002). MLL targets SET domain methyltransferase activity to Hox gene promoters. *Mol. Cell* 10, 1107–1117.
- Ohtani, N., Zebedee, Z., Huot, T.J., Stinson, J.A., Sugimoto, M., Ohashi, Y., Sharrocks, A.D., Peters, G., and Hara, E. (2001). Opposing effects of Ets and Id proteins on p16INK4a expression during cellular senescence. *Nature* 409, 1067–1070.
- Okada, Y., Feng, Q., Lin, Y., Jiang, Q., Li, Y., Coffield, V.M., Su, L., Xu, G., and Zhang, Y. (2005). hDOT1L links histone methylation to leukemogenesis. *Cell* 121, 167–178.
- Reya, T., Morrison, S.J., Clarke, M.F., and Weissman, I.L. (2001). Stem cells, cancer, and cancer stem cells. *Nature* 414, 105–111.
- Rice, K.L., Hormaeche, I., Doulatov, S., Flatow, J.M., Grimwade, D., Mills, K.I., Leiva, M., Ablain, J., Ambardekar, C., McConnell, M.J., et al. (2009). Comprehensive genomic screens identify a role for PLZF-RARalpha as a positive regulator of cell proliferation via direct regulation of c-MYC. *Blood* 114, 5499–5511.
- Sauvageau, M., and Sauvageau, G. (2010). Polycomb group proteins: multi-faceted regulators of somatic stem cells and cancer. *Cell Stem Cell* 7, 299–313.
- Sauvageau, G., Lansdorp, P.M., Eaves, C.J., Hogge, D.E., Dragowska, W.H., Reid, D.S., Largman, C., Lawrence, H.J., and Humphries, R.K. (1994). Differential expression of homeobox genes in functionally distinct CD34+ subpopulations of human bone marrow cells. *Proc. Natl. Acad. Sci. USA* 91, 12223–12227.
- Schuettengruber, B., Chourrout, D., Vervoort, M., Leblanc, B., and Cavalli, G. (2007). Genome regulation by polycomb and trithorax proteins. *Cell* 128, 735–745.
- So, C.W., and Cleary, M.L. (2004). Dimerization: a versatile switch for oncogenesis. *Blood* 104, 919–922.
- So, C.W., Karsunky, H., Passequé, E., Cozzio, A., Weissman, I.L., and Cleary, M.L. (2003). MLL-GAS7 transforms multipotent hematopoietic progenitors and induces mixed lineage leukemias in mice. *Cancer Cell* 3, 161–171.
- So, C.W., Karsunky, H., Wong, P., Weissman, I.L., and Cleary, M.L. (2004). Leukemic transformation of hematopoietic progenitors by MLL-GAS7 in the absence of Hoxa7 or Hoxa9. *Blood* 103, 3192–3199.
- Valk, P.J., Verhaak, R.G., Beijten, M.A., Erpelinck, C.A., Barjesteh van Waalwijk van Doorn-Khosrovani, S., Boer, J.M., Beverloo, H.B., Moorhouse, M.J., van der Spek, P.J., Löwenberg, B., and Delwel, R. (2004). Prognostically useful gene-expression profiles in acute myeloid leukemia. *N. Engl. J. Med.* 350, 1617–1628.
- van der Lugt, N.M., Domen, J., Linders, K., van Roon, M., Robanus-Maandag, E., te Riele, H., van der Valk, M., Deschamps, J., Sofroniew, M., van Lohuizen, M., et al. (1994). Posterior transformation, neurological abnormalities, and severe hematopoietic defects in mice with a targeted deletion of the bmi-1 proto-oncogene. *Genes Dev.* 8, 757–769.
- Verhaak, R.G., Wouters, B.J., Erpelinck, C.A., Abbas, S., Beverloo, H.B., Lugthart, S., Löwenberg, B., Delwel, R., and Valk, P.J. (2009). Prediction of molecular subtypes in acute myeloid leukemia based on gene expression profiling. *Haematologica* 94, 131–134.
- Wong, P., Iwasaki, M., Somerville, T.C., So, C.W., and Cleary, M.L. (2007). Meis1 is an essential and rate-limiting regulator of MLL leukemia stem cell potential. *Genes Dev.* 21, 2762–2774.
- Yeung, J., and So, C.W. (2009). Identification and characterization of hematopoietic stem and progenitor cell populations in mouse bone marrow by flow cytometry. *Methods Mol. Biol.* 538, 301–315.
- Yeung, J., Esposito, M.T., Gandillet, A., Zeisig, B.B., Griessinger, E., Bonnet, D., and So, C.W. (2010). β -Catenin mediates the establishment and drug resistance of MLL leukemic stem cells. *Cancer Cell* 18, 606–618.
- Zeisig, B.B., and So, C.W. (2009). Retroviral/Lentiviral transduction and transformation assay. *Methods Mol. Biol.* 538, 207–229.
- Zeisig, B.B., Kwok, C., Zelent, A., Shankaranarayanan, P., Gronemeyer, H., Dong, S., and So, C.W. (2007). Recruitment of RXR by homotetrameric RARalpha fusion proteins is essential for transformation. *Cancer Cell* 12, 36–51.
- Zeisig, B.B., Cheung, N., Yeung, J., and So, C.W. (2008). Reconstructing the disease model and epigenetic networks for MLL-AF4 leukemia. *Cancer Cell* 14, 345–347.